Earth Planets Space, **58**, 555–567, 2006

Simulations of SH wave scattering due to cracks by the 2-D finite difference method

Yuji Suzuki[1*], Jun Kawahara[2], Taro Okamoto[3], and Kaoru Miyashita[2]

[1]*Graduate School of Science and Engineering, Ibaraki University, Mito 310-8512, Japan*
[2]*Faculty of Science, Ibaraki University, Mito 310-8512, Japan*
[3]*Department of Earth and Planetary Sciences, Tokyo Institute of Technology, Tokyo 152-8551, Japan*

(Received April 5, 2005; Revised October 11, 2005; Accepted October 31, 2005; Online published May 12, 2006)

We simulate SH wave scattering by 2-D parallel cracks using the finite difference method (FDM), instead of the popularly used boundary integral equation method (BIEM). Here special emphasis is put on simplicity; we apply a standard FDM (fourth-order velocity-stress scheme with a staggered grid) to media including traction-free cracks, which are expressed by arrays of grid points with zero traction. Two types of accuracy tests based on comparison with a reliable BIEM, suggest that the present method gives practically sufficient accuracy, except for the wavefields in the vicinity of cracks, which can be well handled if the second-order FDM is used instead. As an application of this method, we also simulate wave propagation in media with randomly distributed cracks of the same length. We experimentally determine the attenuation and velocity dispersion induced by scattering from the synthetic seismograms, using a waveform averaging technique. It is shown that the results are well explained by a theory based on the Foldy approximation for crack densities of up to about 0.1. The presence of a free surface does not affect the validity of the theory. A preliminary experiment also suggests that the validity will not change even for multi-scale cracks.
Key words: Scattering, cracked media, finite difference methods, attenuation, dispersion.

1. Introduction

It is well known that the Earth's interior, especially the lithosphere, has considerably strong short-wavelength heterogeneities that scatter the seismic waves and thereby cause phenomena such as the scattering attenuation, the delay of the arrival times, and the generation of coda waves (e.g., Sato and Fehler, 1998). For revealing the short-wavelength heterogeneous structures in the Earth, it is important to understand theoretically how they act on wavefields.

For this purpose, two types of heterogeneity models are preferably considered; random spatial fluctuations of medium parameters (called random media), and spatial distributions of discrete scatterers such as cracks, inclusions, or cavities. The wave propagation and scattering in media with such heterogeneities have been studied both analytically and numerically. When calculating wavefields in random media, one usually uses domain-type methods, among which the finite difference method (FDM) may be the most popular because of its tractability (e.g., Frankel, 1989; Gibson and Levander, 1990; Jannaud *et al*., 1991a, b; Ikelle *et al*., 1993; Roth and Korn, 1993; Samuelides and Mukerji, 1998; Müller and Shapiro, 2001; Saito *et al*., 2003). In contrast, when dealing with discrete scatterers, boundary-type methods such as the boundary integral equation method (BIEM) has been preferred (e.g., Bouchon, 1987; Coutant, 1989; Benites *et al*., 1992, 1997; Murai *et al*., 1995; Pointer *et al*., 1998; Kelner *et al*., 1999; Liu and Zhang, 2001; Yomogida and Benites, 2002); the application of the FDM is rather restricted (see below as to the references). It may be because the BIEM is generally considered to have advantages over the FDM in the computational accuracy when dealing with discrete heterogeneities (e.g., Benites *et al*., 1992; Liu and Zhang, 2001), and in the great flexibility on the shapes of scatterers. However, the BIEM has also some shortcomings. For example, it cannot easily to be applied to media with discrete scatterers when the surrounding matrices have velocity or density heterogeneities. Moreover, its computational costs rapidly increase with the increasing number of scatterers; its computer program could be also rather hard for beginners to code. Since the FDM is suitable in these points, it is meaningful to apply it to the scattering by discrete scatterers if it gives practically sufficient accuracy with reasonable computational costs. One of the purposes of our study is to clarify this point concerning cracks.

The key to the FDM simulations of scattering by cracks (or fractures) is how we incorporate the cracks into the computational grids. Coates and Schoenberg (1995) proposed a technique in which materials in the grid cells intersected by fractures are modeled by equivalent homogeneous anisotropic materials, on the basis of the theory of Muir *et al*. (1992); here the fractures are modeled by thin weak elastic layers embedded in a surrounding matrix. The merit of

*Now at: Systemlab Corporation, Tokyo 167-0043, Japan.

this technique is that the surfaces of fractures can take arbitrary angles to the grids. It was adopted by Vlastos *et al.* (2003) in their simulations of P-SV wave scattering in 2-D cracked media. Van Baren *et al.* (2001) and van Antwerpen *et al.* (2002) developed another technique in which cracks are replaced by distributed point sources of scattered waves. This is a hybrid method with the BIEM, that is used for evaluating the source. Note that its application is restricted to relatively sparse microcracks, because it neglects multiple scattering and is also based on the long-wavelength approximation. Saenger *et al.* (2000) have expressed cracks by an assembly of the grid points with zero elastic constants and small densities. This is much simpler than the above techniques of crack incorporation and has an advantage in the flexibility on the crack shapes. It requires, however, a rotated staggered grid they proposed to make the computations stable. Using it, Saenger and Shapiro (2002) treated wave propagation in 2-D media with intersecting cracks. Saenger *et al.* (2004) further extended this approach to 3-D cases. Note that Hong and Kennett (2002) also incorporated a fluid-filled crack in the grid in a similar manner, to which their wavelet-based method was applied.

In comparison with the above-mentioned techniques, special emphasis is put on the simplicity of the simulation technique we adopt. Here we treat 2-D SH (or acoustic) wave scattering due to traction-free cracks. For this purpose, we adopt a standard velocity-stress FDM (Virieux, 1984; Levander, 1988). We express cracks just by arrays of grid points with zero traction. Note that this is a natural extension of the simulations of crack propagation based on the velocity-stress FDM originated by Madariaga (1976), in which the boundary conditions on the crack planes can be directly given. Indeed, Fehler and Aki (1978) successfully applied Madariaga's scheme to the diffraction by a single crack in a full space, where they divided the problem into a pair of mixed boundary value problems in half spaces and then solved them. Such a manner, however, has little applicability to many non-coplanar cracks that can be easily treated by the present method. For validating it, we perform two types of accuracy tests based on the comparison with BIEM calculations (Murai *et al.*, 1995). First, we calculate the displacement discontinuity along an isolated crack caused by incident harmonic waves. Second, we synthesize seismograms of waves scattered by clusters of several cracks at distant stations. We then discuss the numerical errors of the FDM calculations, assuming the BIEM counterparts to be exact. We will show that the present method gives practically sufficient accuracy. Note that dealing with 2-D SH waves may not be very practical, but it is our scope to validate the present method sufficiently in such a simple case; the extension to P-SV waves in 2-D cracked media will be given in a later paper.

An interesting topic on cracked media may be the attenuation and velocity dispersion of waves propagating therein. Theoretically, they can be predicted by a stochastic theory based on Foldy's (1945) approximation (Kikuchi, 1981a, b; Yamashita, 1990; Kawahara and Yamashita, 1992; Kawahara, 1992; Zhang and Gross, 1997). This approximation is based on the assumption that many scatterers are distributed randomly and sparsely (Ishimaru, 1978), and it is expected

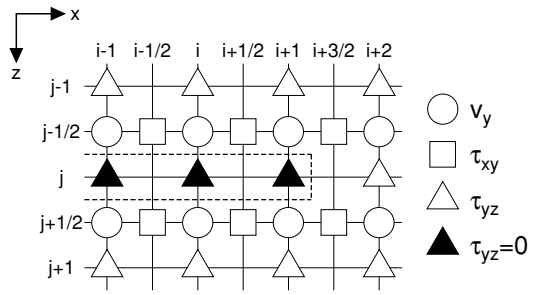

Fig. 1. Staggered grid and implementation of cracks. Antiplane (y-component) velocity and density are defined at the points with circles. Antiplane shear stresses, τ_{xy} and τ_{yz} are defined at the points with squares and triangles, respectively, at both of which rigidity is also defined. The region enclosed by the dotted line corresponds to a crack where the solid triangle denote the points with $\tau_{yz} = 0$.

to give results that are accurate to the first order in the distribution density (Keller, 1964). However, its actual validity limit with respect to the density is not very clear. Using their BIEM, Murai *et al.* (1995) simulated SH wave scattering by 2-D cracks and experimentally determined the scattering attenuation and dispersion, thus validating the Foldy approximation theory as long as the crack density is relatively low (<0.02). Unfortunately, the ordinary peak picking technique as they used in measurement will not work for dense crack distributions, because the initial motions of propagating waves will be often distorted too much to pick the peaks properly. As an application of the present simulation method, we perform here numerical experiments as Murai *et al.* (1995) did, though we adopt an alternative waveform averaging method. We simulate SH wave propagation in media with randomly distributed cracks, and determine the attenuation and dispersion from the spectral changes of averaged seismograms. We show that these parameters are obtained stably, even for rather dense crack distributions, thereby investigating the validity limit of the theory. This is another purpose of this paper and we will show that the theory remains valid, even for considerably high crack densities.

This paper is organized as follows. In the next section, we outline the FDM that we adopt, including the implementation of cracks. We validate the method in Section 3 through the two accuracy tests. On the basis of the numerical experiments using it, we then investigate the validity of the Foldy approximation theory in Sections 4 and 5; the former section is focused on the validity limit of the theory, assuming identical cracks, whereas the latter concerns cracks with variable lengths. A discussion and conclusions are presented in the last section.

2. Finite Difference Method

We adopt a velocity-stress finite difference scheme for 2-D SH waves with the accuracy of fourth order in space and second order in time in most simulations. It is a straightforward extension of Virieux's (1984) second-order scheme for SH waves after Levander's (1988) fourth-order scheme for P-SV waves. In some cases, we also use Virieux's original second-order scheme for comparison. Their algorithm is so standard that it is not detailed; we just illustrate a stag-

gered grid (Fig. 1). Here the x-, y- and z-axes are taken in the horizontal, antiplane, and vertical directions, respectively. Note that the grid spacings in the x- and z-directions are assumed to have the same length Δh.

We assume that any crack is horizontal (parallel to the x-axis) and traction-free and is incorporated into the grid just by imposing the shear stress $\tau_{yz} = 0$ on the horizontally arrayed grid points (Fig. 1). As mentioned in Section 1, this may be analogous to the method of Fehler and Aki (1978) in that a Neumann problem is explicitly set; although they transformed the problem into a pair of mixed problems, we solve it in a straightforward way. We define the crack tips as the leftmost and rightmost points of the array (e.g., the grid point $(i + 1, j)$ in Fig. 1); though it may be also possible to define them as the positions half a grid spacing outside these grid points (e.g., $(i + 3/2, j)$), it is confirmed that the difference is negligible for sufficiently small grid spacings as expected.

In any simulation performed, a plane wavelet is assumed to propagate upward (in the negative z-direction) from below and be normally incident on cracks. Then velocity seismograms are synthesized at specified grid points, which are finally integrated with the trapezoidal rule to yield the displacement seismograms. Concerning the artificial boundaries of the whole grid (model space), we again impose simple conditions. The cyclic boundary condition is applied to the left and right ends to approximately express an infinitely long cracked layer. A standard absorbing boundary condition of Clayton and Engquist (1977) is assumed along the bottom end. The condition of the top end is chosen between the absorbing or traction-free boundary conditions, depending on simulations. Although artificial reflections from the absorbing boundaries cannot be perfectly erased, we actually analyze the portions of seismograms not contaminated with them.

Hereafter, the shear wave velocity and the density of the background material, β and ρ, are set to be unity. We also assume that all the cracks have the same half length $a = 1$, except in Section 5 where we consider a distribution of crack lengths. The values of other parameters are normalized with them. The grid spacing Δh are chosen to satisfy the ordinary sampling criterion

$$\Delta h < \beta / n f_{ul}, \tag{1}$$

where n is 5 and 10 for the fourth- and second-order schemes, respectively, and f_{ul} is the effective upper limit of the frequency band of waves.

3. Accuracy Tests

3.1 Crack displacement discontinuity

In this section, we compare the results of our FDM simulations with those given with the frequency-domain BIEM of Murai *et al.* (1995), thus trying to validate the present method. In order to treat the results of the BIEM as the correct answers, we pay special attention to their accuracy; i.e., we discretize the crack planes finely so that the discretization interval Δs in the BIEM may be much smaller than not only the crack length and the wavelength but also the distances between neighboring cracks (namely, the minimum distance between two crack planes). Actually, we choose $\Delta s = 0.0025a$. In the first test, we check the validity of the present method through calculation of displacement discontinuity along a single crack, caused by the normal incidence of harmonic SH waves. This was analytically solved by Mal (1970), whose results have often been used by several authors to validate their own BIEM. Yamashita (1990), among others, developed a BIEM algorithm for treating an isolated crack, which reproduces Mal's results quite accurately. It was extended by Murai *et al.* (1995) to treat many cracks. Its code is used here.

Now let us calculate the results corresponding to Mal's (1970) using the present FDM. Consider an isolated crack with the length $2a$, upon which a quasi-monochromatic wave train

$$u^0(x, z, t) = H(kz + \omega t) \sin(kz + \omega t) \tag{2}$$

normally impinges; here $\omega = 2\pi f$, f is the frequency, $k = \omega/\beta$ is the wavenumber, and $H(\ )$ is the step function. This causes the oscillation of the crack faces, and approaches the stationary state with the lapse time. We evaluate the amplitudes of the oscillatory displacement discontinuity along the crack when the oscillation appears almost stationary. Since the displacement discontinuity cannot be defined on the crack plane, we measure instead the differences of the displacement seismograms calculated at the pairs of grid points just above and below the crack plane (e.g., the grid points $(i, j \pm 1/2)$ in Fig. 1), and then take their amplitudes. The approximation errors due to the offsets of the measurement points from the crack plane would be small if Δh is sufficiently small.

The results are summarized in Fig. 2(a), where the cases of the normalized wavenumber $ka = 1.0$, 2.8, 4.2, and 6.0 are examined after Mal (1970); the corresponding wavelengths are $6.3a$, $2.2a$, $1.5a$, and $1.0a$, respectively. Here we set $\Delta t = 0.003$ (in unit of a/β) and impose the absorbing boundary condition on the top end of the grid. On the basis of the fourth-order finite difference scheme, we repeatedly calculate the crack displacement discontinuity with $\Delta h/a = 0.05$, 0.025, and 0.0125. Note that the corresponding results using the BIEM agree well with Mal's. One might expect that the FDM results may approach the BIEM results (i.e., the exact solutions) as $\Delta h/a$ decreases; instead, they appear to converge on somewhat (several percents) smaller values on the whole. This may not be surprising if the nonlocality of the fourth-order finite difference operator is considered, that is, the calculation of the particle velocity at a grid point (e.g., $(i, j + 1/2)$ in Fig. 1) requires the stresses at the preceding time at, not only the neighboring points $((i, j), (i, j+1)$ and $(i \pm 1/2, j+1/2))$, but also the points beyond them $((i, j - 1), (i, j + 2)$ and $(i \pm 3/2, j+1/2))$. This means that the operator acts across the crack plane when the particle velocity is calculated at its very vicinity, resulting in errors. [As an aside, the nonvanishing displacement discontinuity at a distance larger than 1.0 in Fig. 2(a) can be explained by the offsets of the measurement points from the crack plane, and therefore gets smaller for smaller Δh]. Such a problem would not occur when the more local second-order operator is adopted, that never crosses the crack plane. We confirm it by recalculating the displacement discontinuity using the second-order

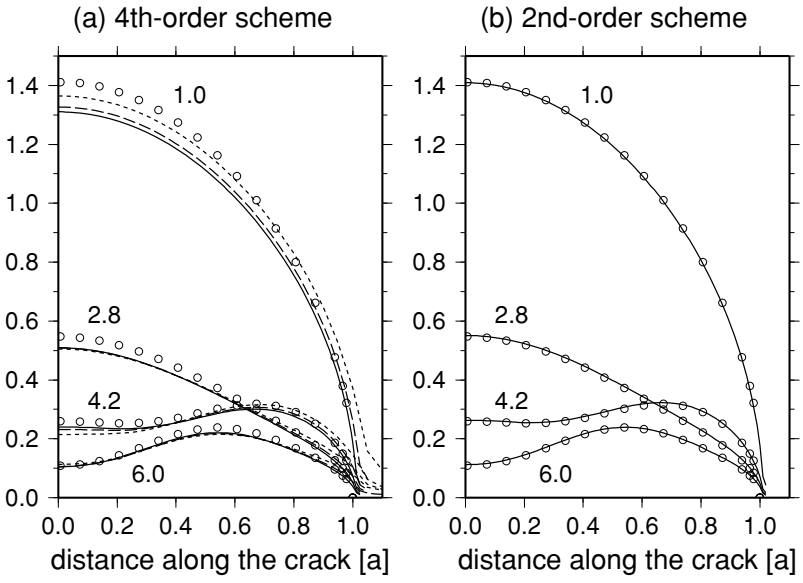

Fig. 2. Displacement discontinuity along a single crack due to normal incidence of harmonic SH waves, normalized with respect to the value at the center of the crack at $ka \to 0$. The abscissas represent the distance from the center (in unit of a). The curve parameters denote ka. The open circles indicate the calculations by the BIEM of Murai *et al.* (1995), whereas the lines do the FDM calculations. (a) The solid, dashed, and dotted lines denote the calculations by the fourth-order scheme with $\Delta h/a = 0.0125$, 0.025, and 0.05, respectively. (b) The solid lines denote the calculations by the second-order scheme with $\Delta h/a = 0.01$.

scheme. Now we assume that $\Delta t = 0.00125\ (a/\beta)$ and $\Delta h = 0.01a$. The results are indeed shown to agree with the BIEM calculations almost perfectly (Fig. 2(b)), supporting the above discussion.

In summary, it is shown that crack displacement discontinuity, or wavefields in the vicinity of cracks, can be quite accurately evaluated using the second-order FDM. On the other hand, the fourth-order FDM systematically underestimates them, even for considerably small grid spacing, because of the nonlocality of the finite difference operator. The relative errors, however, are several percents at most. If they are tolerable, the fourth-order FDM may be useful because of the lower computational costs due to its numerical dispersion behavior better than that of the second-order one.

3.2 Scattered waveforms due to clustered cracks

In the second test, we synthesize the displacement seismograms of scattered waves by clustered several cracks and examine the numerical errors. Here we adopt the fourth-order FDM only. We locate the cracks rather closely (with the intervals not very larger than Δh) to see the effect on the accuracy of multiple scattering that would be strongly excited under such situations. In contrast, the observation points (hereafter, called stations) are located not very close to the cracks (with the distance larger than $2a$), since the inaccuracy of "near-field" displacement calculated by the fourth-order FDM has been demonstrated in the above subsection.

In the following, we set $\Delta t = 0.005\ (a/\beta)$ and $\Delta h = 0.025a$ throughout; the absorbing boundary condition is again imposed on the top end of a grid (model space). Small numbers of cracks are closely located at around the center of the grid, and a plane wavelet is assumed to impinge on the cracks from below. Here we adopt a Ricker wavelet (second derivative of a Gaussian function; see Murai *et al.*, 1995 for details), with the dominant frequency $f_c = 0.6$ (in unit of β/a) corresponding to $ka = 3.77$; here the corresponding wavelength $\lambda_c = 1.67a$ is close to the crack length so that scattering would occur strongly. We then synthesize the seismograms at horizontally arrayed stations above the cracks.

First, we treat a single crack for reference as shown in Fig. 3(a). Note that the center of the crack is located at $(x, z) = (10a, 6.25a)$, defining the origin as the top left corner of the area. We evenly space 101 stations between $(x, z) = (0, 0)$ and $(0, 20a)$, among which the stations at $(x, z) = (0, 0)$, $(5a, 0)$ and $(10a, 0)$ are termed S_3, S_2 and S_1, respectively. The FDM as well as BIEM seismograms obtained at these three stations are depicted by Figs. 3(b) to 3(d). It is demonstrated that the single-scattered waves with relatively short durations follow the incident wavelets. They are separately recognized at the horizontally distant station S_3, whereas they overlap at S_1 right above the crack, resulting in the deformation of the Ricker wavelet. In each case, the agreement between both seismograms is quite satisfactory, in spite of the discrepancy observed at the vicinity of cracks (Fig. 2(a)). This suggests that the errors due to the nonlocal finite difference operator would not strongly affect the "far-field" displacement. In order to closely look into the difference between the FDM and BIEM traces, we define here a normalized residual trace as

$$R(t) = \left[u^{\mathrm{FDM}}(t) - u^{\mathrm{BIEM}}(t)\right] / \max\left|u^{\mathrm{BIEM}}(t)\right|, \qquad (3)$$

where u^{FDM} and u^{BIEM} are the FDM and BIEM traces, respectively.

Note that the time steps of both traces were originally different; we therefore cubic spline-interpolated the FDM traces and then resampled them to match the BIEM traces. Figure 3(e) denotes the gather of the residual traces at all the stations. Considering the BIEM traces to be correct, we

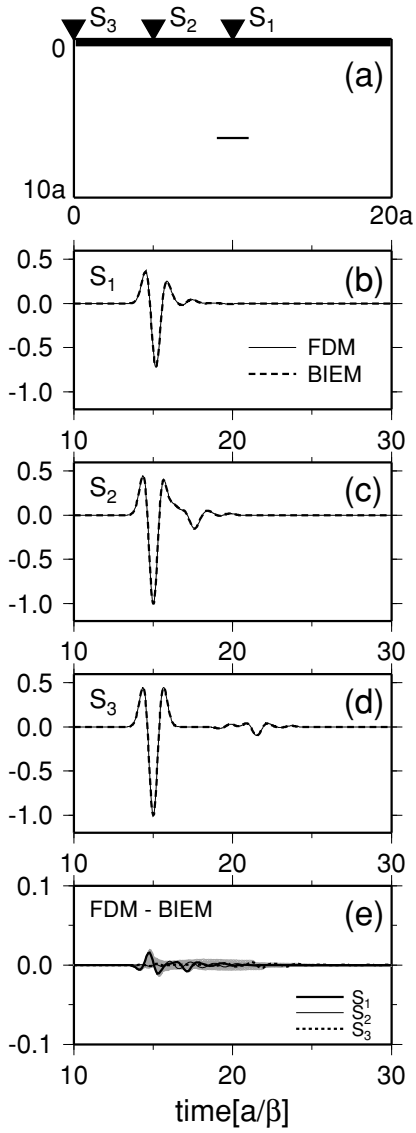

Fig. 3. Comparison of seismograms based on the FDM and BIEM simulations. (a) Geometry of the simulation model examined. Here a single crack is located, above which 101 stations are horizontally spaced (the thick horizontal line). Note that $\Delta h = 0.025a$. (b) FDM and BIEM traces at the station S_1, indicated in (a), normalized with the maximum amplitude of the initial wavelet. (c) As for (b) except for the station S_2. (d) As for (b) except for the station S_3. (e) Residual traces (difference between the FDM and BIEM traces). The thick solid, thin solid and dotted lines denote the residuals at S_1, S_2 and S_3, respectively. Residuals at all the other stations are indicated by the cloud of the fine gray lines.

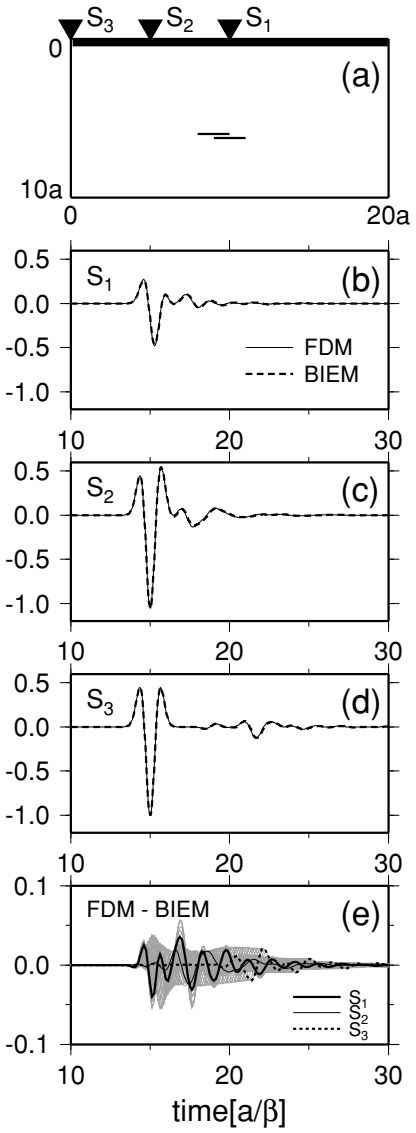

Fig. 4. Same as those in Fig. 3, except for two cracks closely located with the vertical interval $0.25a$.

may remark that the relative errors of the FDM traces are about 2% at most and, hence, considerably small.

Next, we add one more crack at $(x, z) = (9a, 6a)$, where the interval between the cracks in the vertical direction is $0.25a = 10\Delta h = 0.15\lambda_c$ (Fig. 4(a)). This results in long wave trains after the single-scattered waves, reflecting the reverberation between the cracks (Figs. 4(b) to 4(d)). Although the FDM and BIEM traces agree well, the amplitudes of the residual traces are rather larger than before (compare Fig. 4(e) with Fig. 3(e)). Careful observation of the traces in Figs. 4(b) to 4(d) suggests that these errors are mainly attributed to the slight phase offsets between the traces; except for these offsets, the errors in amplitude are still quite small. To see the effect of the interval between the cracks on the FDM accuracy, we also reexamine the same model, except that the center of the upper crack is relocated at $(x, z) = (9a, 4.25a)$, with the vertical interval $2a = 80\Delta h = 1.2\lambda_c$ (Fig. 5(a)). Comparison of Figs. 4(b) to 4(d) with Figs. 5(b) to 5(d) shows that the longer crack interval results in a somewhat longer duration of the reverberation. Figures 4(e) and 5(e) suggest, however, that the FDM errors appear roughly unchanged, especially for the later waves. Concerning the direct waves, the errors are somewhat amplified at some stations (as S_1).

We finally examine the case of 10 cracks closely spaced with vertical intervals $\geq 0.25a$, as depicted by Fig. 6(a). In this case, we observe a large number of wave trains, which are interpreted as coda waves excited by strong multiple scattering (Figs. 6(b) to 6(d)). Here a small but perceptible discrepancy is observed between the FDM and BIDM traces in some portions of the late coda; the normalized residuals exceed 10% at the maximum (Fig. 6(e)). Nevertheless, the apparent coincidence of both traces is still fairly good. Note

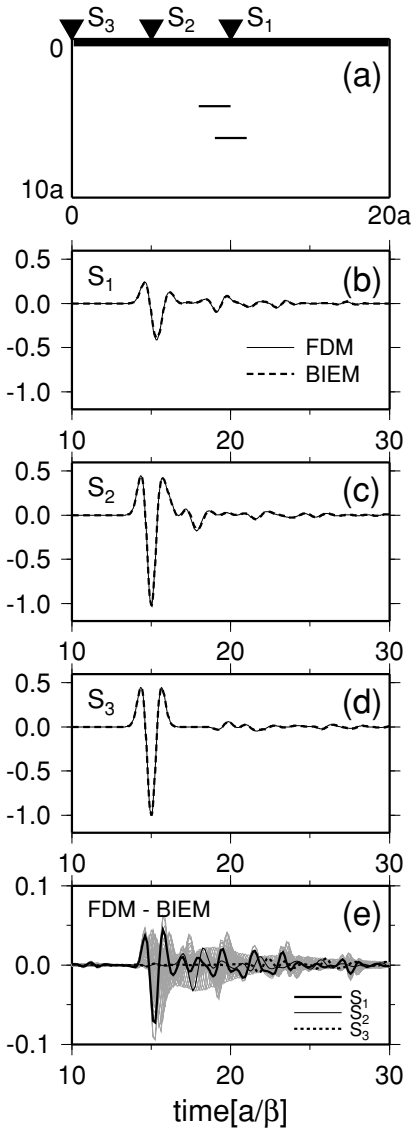

Fig. 5. Same as those in Fig. 3, except for two cracks located with the vertical interval $2a$.

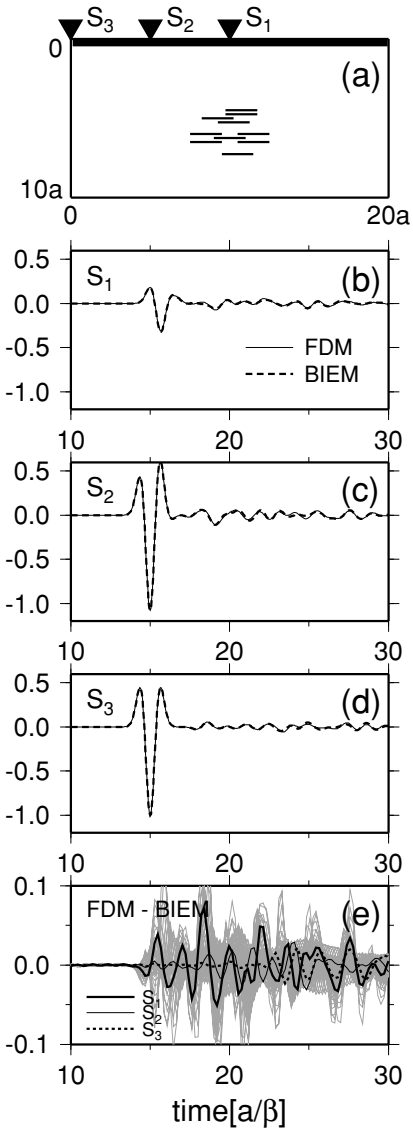

Fig. 6. Same as those in Fig. 3, except for 10 cracks closely clustered with the minimum vertical interval $0.25a$.

that $\max|u^{\mathrm{BIEM}}(t)|$ in Eq. (3) (mostly, the amplitudes of the direct waves) largely varies with the stations (Figs. 6(b) to 6(d)). This would be responsible for the large spatial variation of the residuals shown in Fig. 6(e).

In summary, the fourth-order FDM generally gives considerably accurate seismograms (except for the vicinity of cracks), especially concerning the direct and early coda waves. The overall agreement between the FDM and BIEM (or correct) traces seems to be successful, though the relative errors tend to somewhat increase with the increasing number of cracks (Figs. 3(e) to 6(e)). Moreover, the dependence of the errors on the intervals between cracks appears much weaker. These characteristics would be preferable, especially when one deals with scattering by a large number of densely distributed cracks. Although we did not thoroughly pursue it here, the accuracy might be improved if the second-order FDM is totally adopted to the cracked media. In that case, however, we will probably need to use smaller grid spacings than those used in the present paper, because the second-order FDM is less accurate concerning the crack-free regions, due to its poorer numerical dispersion relation.

We also point out that the FDM may be more cost-effective than the BIEM in treating many cracks, because the latter's costs rapidly increase as the number of cracks increases, whereas the former's costs are essentially unchanged (depending on the grid size instead). This is illustrated by a side experiment (not shown), where Δs was taken to be five times larger than in the above experiments (i.e., $\Delta s = \Delta h/2 = 0.0125a$). It reduced the accuracy of the BIEM traces to the same level as for the FDM traces but remarkably saved the costs. Even then, the present BIEM needed larger CPU times than the FDM when more than 10 cracks were treated. This suggests the practicability of the present simulation method from the viewpoints of costs as well as of accuracy.

4. Validation of the Foldy Approximation Theory

In this section, we show an example of the application of the present simulation method, whose accuracy has been

confirmed above. Using the method, we investigate here the validity of the Foldy approximation theory of Kawahara and Yamashita (1992) that predicts the scattering attenuation and velocity dispersion of elastic waves in 2-D media with identical parallel cracks. Here the prediction is stochastic in a sense that the theory is based on the mean wave formalism, i.e., it treats the ensemble average of real wavefields. Note that the theory also adopts an approximation in which the waves effectively impinging on each scatterer (crack) are equal to the waves that would be observed without the scatterer. This approximation, first introduced by Foldy (1945), yields a closed equation for mean waves (called the Foldy–Twersky integral equation; Ishimaru, 1978); Kawahara and Yamashita (1992) solved it to obtain the attenuation and phase velocity of the mean waves to the first order in the crack density. The approximation is sometimes considered as a kind of single scattering approximation, since it does not take account of interactions between scatterers explicitly.

A similar trial to validate the theory of Kawahara and Yamashita (1992) was done by Murai *et al.* (1995) on the basis of a peak picking technique, in which the attenuation and phase velocity are determined from the amplitudes and travel times of the maximum peaks of bandpass-filtered seismograms and then averaged. Although the peak picking technique is simple and practical in real seismic observations, it also has some shortcomings. One of them is its less applicability to dense crack distributions, as mentioned in Section 1. In addition, its results depend on the choice of filter bandwidths. Another popular method may be to stack the amplitude spectra of individual seismograms, thereby estimating the averaged spectral change (e.g., Roth and Korn, 1993). The results, however, now depend on the time windows used for Fourier-transforming the seismograms, since no window perfectly separates the direct wave components from the seismograms. We also notice that none of these methods are conceptually consistent with the mean wave formalism. To overcome these problems, we adopt an alternative waveform-averaging method loyal to the formalism, as stated below.

First, we assume N cracks with the length $2a$ inside a rectangular area with the horizontal size W and vertical size L. Using a uniform random number series, the cracks are distributed inside the area almost randomly, except for the non-overlapping constraint that the interval between any two points belonging, respectively, to any two crack planes must be greater than $0.25a$. Here the 2-D crack density is defined as $\epsilon = Na^2/WL$. Second, we array 100 stations evenly along a horizontal line $2a$ above the top end of the crack distribution area. We then let a plane wavelet be vertically incident on the bottom end from below, and synthesize seismograms at the stations using the FDM. We adopt here an incident wavelet with the following source time function (first derivative of a Gaussian function; see Fig. 7):

$$u^0(t) = -4\pi t \mathrm{e}^{-2\pi t^2}, \tag{4}$$

whose amplitude spectrum is

$$F(\omega) = \frac{\omega}{\sqrt{2}} \mathrm{e}^{-\omega^2/8\pi}. \tag{5}$$

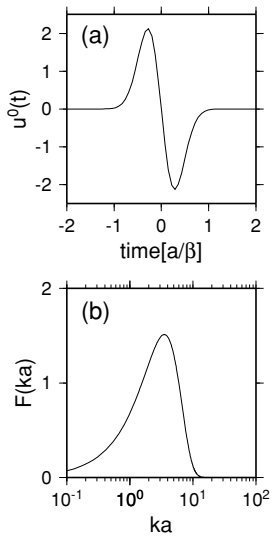

Fig. 7. (a) Source time function of the incident wavelet used. The abscissa denotes time in unit of a/β. (b) Amplitude spectrum of the wavelet as a function of normalized wavenumber $ka = \omega a/\beta$.

This is because the present wavelet has a broader spectral band than that of the Ricker wavelet, being more effective for the present purpose. We then repeat the above simulation for N_D different realizations of the crack distribution that are stochastically identical but are generated using different random number series. Third, we average all the seismograms obtained for each realization. This means that spatial averaging is substituted for ensemble averaging, assuming ergodicity. The results are then ensemble-averaged over the N_D realizations of the crack distribution; the final result is termed "synthetic mean wave". Fourth, the spectrum of the mean wave is calculated. In doing this, we select a time window that effectively includes the whole mean wave. If sufficiently many seismograms are stacked, the incoherent coda waves will be removed almost completely and, hence, the window width will not influence the results; actually, we choose N_D enough to achieve this state. We then evaluate the attenuation Q^{-1} and the phase velocity v from the spectral ratio, $C(f)$, of the mean wave to the initial wavelet that would be observed without the cracks. After some calculation, we obtain

$$C(\omega) = \exp\left[i\omega L\left(\frac{1}{v} - \frac{1}{\beta}\right) - \frac{\omega L}{2vQ}\right], \tag{6}$$

and, hence,

$$\frac{1}{v} = \frac{1}{\beta} + \frac{1}{\omega L}\tan^{-1}\frac{\mathrm{Im}C}{\mathrm{Re}C}, \tag{7}$$

$$Q^{-1} = -\frac{2v}{\omega L}\log|C|, \tag{8}$$

where "Im" and "Re" denote the imaginary and real parts, respectively. Practically, we evaluate them only for some frequency band inside which the initial wavelet has sufficiently high energy for accurate calculation. A disadvantage of the method is that it is not straightforward to explicitly evaluate the estimation errors of Q^{-1} and v. Instead, we calculate the standard deviation of the synthetic mean

Table 1. Parameters of the crack distribution models used in simulations. BC indicates the boundary condition on the top end of the grid. AB indicates an absorbing boundary being settled above the station array. FS indicates a free surface being settled along the array.

Model	N	$W \times L$	ϵ	N_D	BC
1	20	$40a \times 38a$	0.013	6	AB
2	40	$40a \times 38a$	0.026	9	AB
3	40	$40a \times 18a$	0.056	12	AB
4	32	$40a \times 8a$	0.1	18	AB
5	40	$40a \times 5a$	0.2	18	AB
4a	32	$40a \times 8a$	0.1	18	FS

wave and regard it as the estimation error. We also compute the waveform predicted by the Foldy approximation theory ("predicted mean wave"), using Eq. (6) with Q^{-1} and v given by the theory and then inverse Fourier-transforming. If the predicted mean wave coincides with the synthetic one within the error range, we regard their coincidence as significant.

In the following, we choose $\Delta t = 0.005\ (a/\beta)$ and $\Delta h = 0.025a$ throughout. Other parameters of the crack distribution models used are summarized in Table 1. An example of the realizations for each crack distribution model is depicted in Fig. 8.

We first demonstrate the results for Model 1 (Fig. 9), that is, the case where the crack density ($\epsilon = 0.013$) is so low that the Foldy approximation is expected to be valid. In Fig. 9(a), we plot $N_D \times 100$ seismograms used in the analysis. Here we also show the trace of the synthetic mean wave and its standard deviation (error range) derived from the seismograms; the initial wavelet without the cracks is also plotted for reference (see also Fig. 9(b) as the close-up). Here one may clearly observe the attenuation on the direct wave part of the mean wave trace ($44 < t < 46$ in unit of a/β). The direct wave is also followed by a pulse of relatively long duration (around $46 < t < 50$). However, the trace does not contain a coda-like long wave train, implying that the averaging process is successful in removing coda waves. We further plot the trace of the predicted mean wave in the figure. The coincidence of the synthetic and predicted mean waves is considerably good. This also suggests that the above-mentioned pulse, after the direct wave, should result from the waveform dispersion of the initial wavelet due to scattering. The values of Q^{-1} and $\Delta v/\beta$ derived from the both traces are plotted in Figs. 9(c) and 9(d) for $0.5 < ka < 10$ ($k = \omega/\beta$), respectively, where $\Delta v = \beta - v$ is the phase velocity reduction due to scattering. The agreement between the experimental and theoretical values are fairly good on the whole, even including the ripple pattern of $\Delta v/\beta$ for high wavenumbers, as may be expected from the above results. It may strongly support the validity of the Foldy approximation theory on cracked media, being consistent with the results of Murai *et al.* (1995).

We next show the results for the models with denser distributions (Models 2 to 5), focusing on the validity limit of the theory. Here, however, we skip the result for Model 2

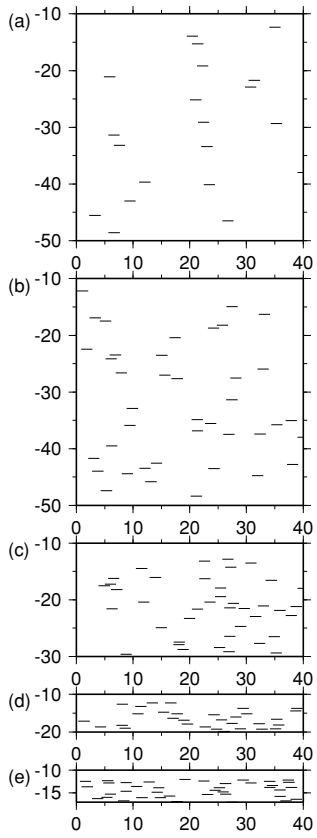

Fig. 8. Examples of crack distribution realizations for (a) Models 1 ($\epsilon = 0.013$), (b) 2 ($\epsilon = 0.026$), (c) 3 ($\epsilon = 0.055$), (d) 4 ($\epsilon = 0.1$), and (e) 5 ($\epsilon = 0.2$). The axes denote length normalized with a. 100 stations are evenly spaced along the top end of each rectangular region, just below which is a gap with the thickness $2a$ between the stations and the really cracked area.

($\epsilon = 0.026$), since it is almost the same as that for Model 1. The results for Models 3 and 4 with a relatively dense distribution ($\epsilon = 0.056$ and 0.1) are shown in Figs. 10 and 11, respectively, where we may still recognize the fairly good agreement between the synthetic and theoretical results in both the traces (Figs. 10(a), 11(a)) and Q^{-1} and $\Delta v/\beta$ (Figs. 10(b), 10(c), 11(b), 11(c)). Concerning the more denser distribution (Model 5, $\epsilon = 0.2$), however, we observe a clear discrepancy, as shown in Fig. 12. Here the predicted values of Q^{-1} and $\Delta v/\beta$ systematically overestimate the measurements for $ka < 1$. This may be partly attributed to the effect of multiple scattering among closely located scatterers. As stated in Section 1, the Foldy approximation is based on the randomness and sparseness of scatterer distributions. Strictly speaking, however, a distribution of non-overlapping scatterers cannot be perfectly random for finite distribution densities. In the present case, with such a dense distribution, the randomness would be largely degraded and result in large approximation errors. Indeed, a more rigorous treatment of mean waves revealed that the terms of order ϵ^2, neglected by Kawahara and Yamashita (1992), can be described in terms of such nonrandomness (Keller, 1964). Another possible reason for the discrepancy may be the inappropriate definition of Q for strongly attenuated waves. In the theory as well as the measurement, we assume the exponential decay expressed by

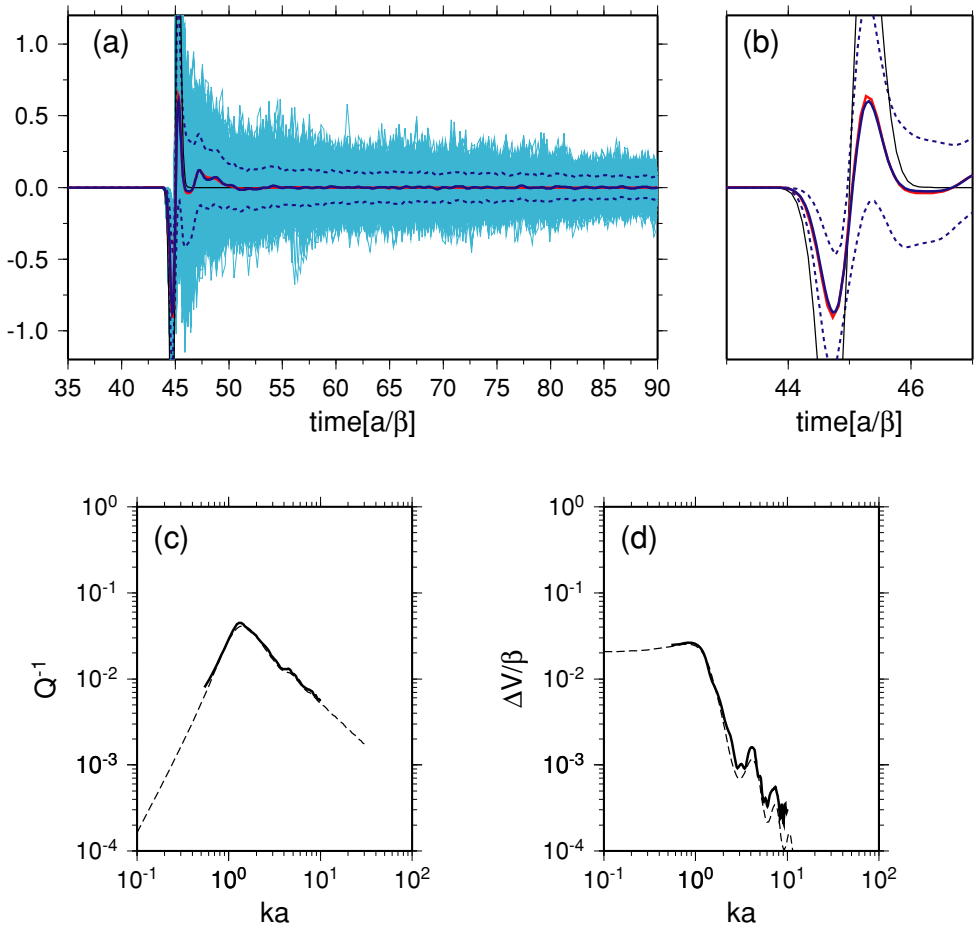

Fig. 9. (a) Seismograms obtained for Model 1 ($\epsilon = 0.013$). The cloud of thin light blue lines denotes all the synthetic seismograms. The solid blue curve indicates the synthetic mean wave, and the dotted blue curves do its standard deviation. The predicted mean wave is indicated by the red curve, though almost masked by the solid blue one. The thin black curve denotes the initial wavelet that would be observed without the cracks. (b) The close-up of the direct wave part in (a). The synthetic seismograms are omitted. (c) Q^{-1} for the synthetic seismograms (thick solid curve). The prediction by the Foldy approximation theory is denoted by the dashed curve. (d) As for (d), except for $\Delta v/\beta$, where Δv is the phase velocity reduction.

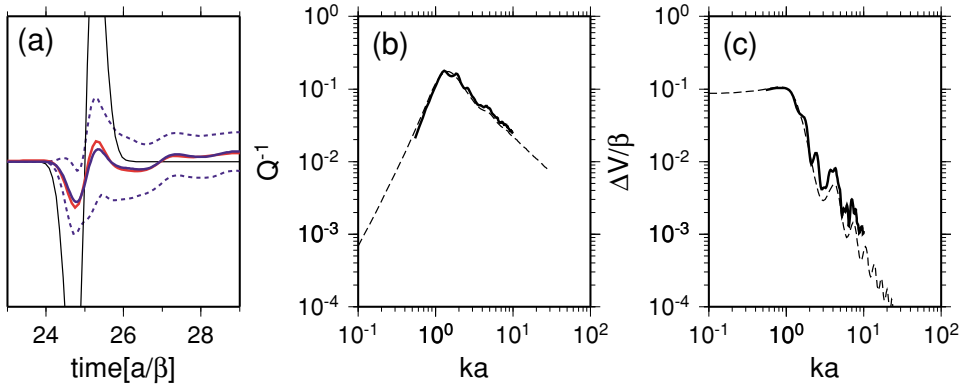

Fig. 10. Same as those in Fig. 9 except for Model 3 ($\epsilon = 0.056$). The seismograms in the full range as Fig. 9(a) is omitted.

$\exp(-kQ^{-1}x/2)$ as usual, where x is the travel distance. Strictly, however, it is an approximation valid for weak attenuation, i.e., $Q^{-1} \ll 1$ (e.g., Aki and Richards, 2002). This will not be satisfied in the present case, where the maximum value of Q^{-1} approximates to 1, probably making both the theory and measurement less reliable. This inference appears to be supported by the distinct acausal motion of the predicted mean wave before the onset of the initial wavelet without cracks ($t \sim 11$), which deviates from the error range of the synthetic mean wave (Fig. 12(a)).

Finally, we investigate the effect of a free surface on the attenuation and dispersion. For the purpose, we reexamine the same model as Model 4, except that the stations are located on the free surface, termed Model 4a. The results for the model is shown in Fig. 13. Here the theoretical results are essentially unchanged, except that the amplitude

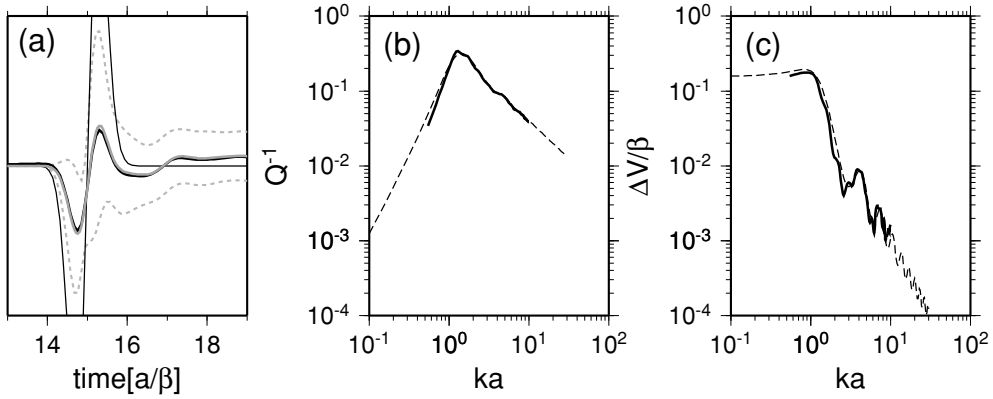

Fig. 11. Same as those in Fig. 10 except for Model 4 ($\epsilon = 0.1$) as well as monochromatic drawing. In (a), the synthetic mean wave and its standard deviation are now indicated by gray lines, whereas the predicted mean wave is done by bold black line.

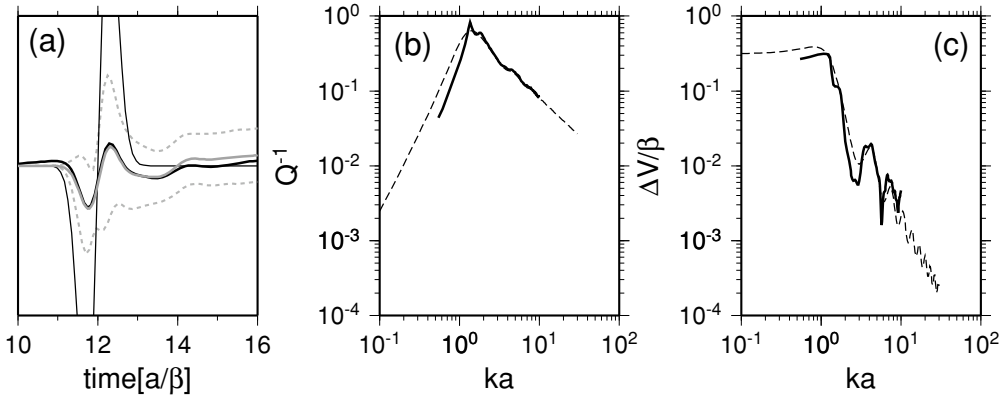

Fig. 12. Same as those in Fig. 11 except for Model 5 ($\epsilon = 0.2$).

of the predicted mean wave (as well as the initial wavelet without cracks) is exactly duplicated on the surface. We also observe the experimental results similar to those for Model 4 (Fig. 11) on the whole. A noticeable difference is that the measured $\Delta v/\beta$ are not stably determined for high wavenumbers. This may reflect the fact that the high-frequency coda waves are not sufficiently removed in this case, even though we assume here $N_D = 18$ as before (see the ripples of the coda part of the synthetic mean wave for Model 4a, not seen for Model 4 (Fig. 13(d))). The amplitude of the direct waveform of the synthetic mean wave is also slightly different from that for Model 4, corresponding to the slightly larger values of the measured Q^{-1} in the dominant wavenumber range $0.2 < ka < 0.5$. Such discrepancies should be regarded as the effects of a free surface, since any other conditions are unchanged, though they are rather small so that they are negligible.

In summary, one may say that the theory is valid for crack densities up to about 0.1 but probably not beyond it. The presence of a free surface does not change the conclusion. We remark that the real (though 3-D) crack densities of the crustal rock inferred from the shear-wave splitting analyses do not generally exceed 0.1, except for regions under some special conditions such as very near-surface layers or tectonically active regions (Crampin, 1994). We may therefore infer that the Foldy approximation theory may be applicable to most regions of the Earth's crust, though more accurate statements would require the researches on scattering in 3-D cracked media.

5. Scattering Due to Cracks with Binary Lengths

Up to now, we have assumed the distributions of cracks identical except for the locations, as Murai *et al.* (1995) did. This assumption, however, may be too simple to model the real crustal cracks or fractures, which are generally multi-scale with a fractal nature (e.g., Main *et al.*, 1990). The present FDM would be useful in dealing with such multi-scale crack systems because its application will be straightforward, in contrast to the BIEM of Murai *et al.* (1995) that would require a significant amount of modification to be applied. Here we just carry out a preliminary experiment; we simulate the scattering by cracks with binary lengths using the FDM. We then evaluate the attenuation and dispersion and compare them with the predictions of the Foldy approximation theory, as in the preceding section. Note that Yamashita (1990) dealt with the attenuation and dispersion due to scattering by cracks whose lengths obey a band-limited power law distribution. He directly solved the Foldy–Twersky integral equation that includes the integral with respect to the crack length in this case, using a technique in which the equation is transformed to a pair of differential equations. Instead of such a rather laborious manner, we assume a simple superposition principle; we just sum up the values of Q^{-1} or $\Delta v/\beta$ for the subgroups com-

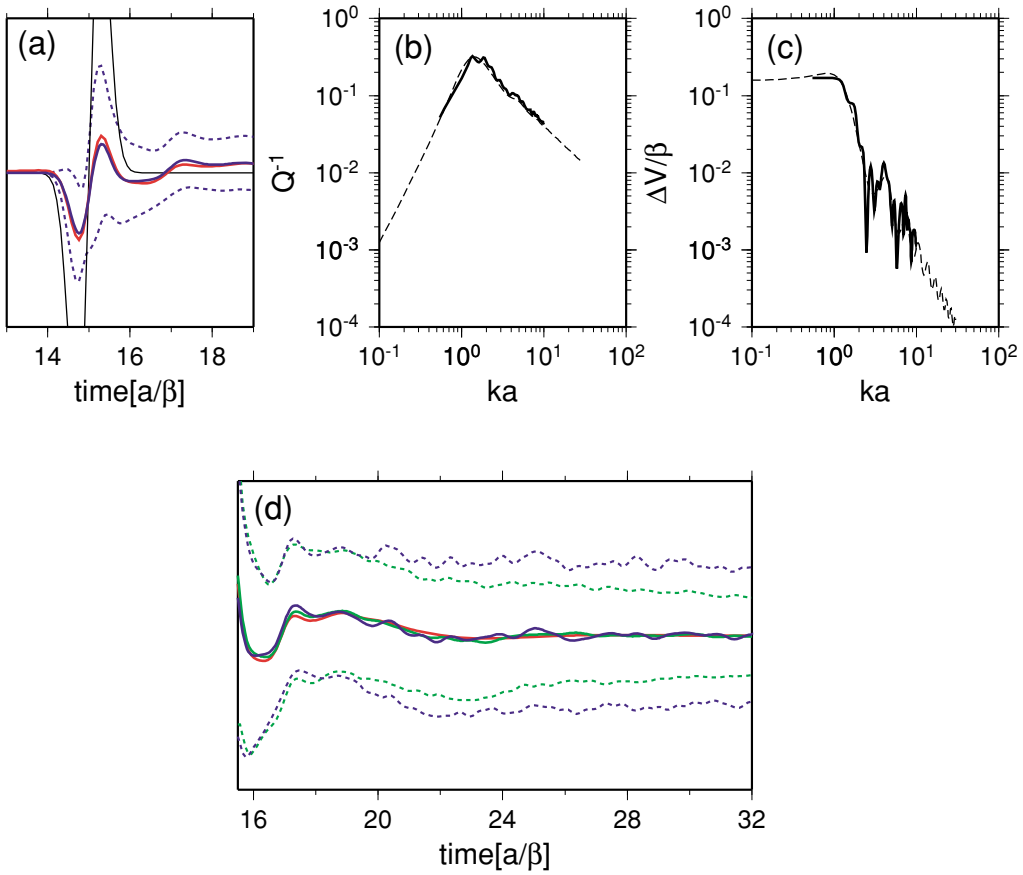

Fig. 13. Effect of a free surface. (a) to (c) are the same as for Figs. 10(a) to (c), except for Model 4a (Model 4 plus the free surface). (d) indicates the comparison among the coda traces for Models 4 (green curves), Models 4a (blue curves) and the corresponding predicted mean wave (red curve). The meanings of the solid and dotted curves are the same as for (a).

posed of identical cracks. This should be valid as long as the crack density is so low that one can neglect the higher-order terms in the crack density (e.g., Hudson, 1986).

We consider a random distribution of parallel cracks that are divided into two subgroups, each of which contains N_j cracks with the length $2l_j a$ ($j = 1, 2$), where a is now a reference scale. Letting the distribution area be $W \times L$ again, one may define the crack density in this case as

$$\epsilon = \sum_{j=1}^{2} \epsilon_j, \quad \epsilon_j = \frac{N_j (l_j a)^2}{WL}. \tag{9}$$

Then the theoretical predictions of the attenuation and dispersion may be given as

$$Q^{-1}(ka) = \sum_{j=1}^{2} \epsilon_j \hat{Q}(kl_j a), \quad \frac{\Delta v}{\beta} = \sum_{j=1}^{2} \epsilon_j \frac{\Delta \hat{v}(kl_j a)}{\beta}, \tag{10}$$

where the caret means a prediction for identical cracks distributed with unit crack density. We assume here that $N_1 = 32$, $N_2 = 12$, and $l_1/l_2 = 1/2$; assigning a to the mean crack length, then $l_1 = 11/14$ and $l_2 = 11/7$. We choose the same values of W, L, Δt and Δh as for Model 1; thereby the crack density is also the same ($\epsilon = 0.013$). Concerning the boundary conditions and the values of N_D, however, they are set as for Model 4a. We term this simulation model as Model 6; an example of the crack distribution realization is depicted in Fig. 14.

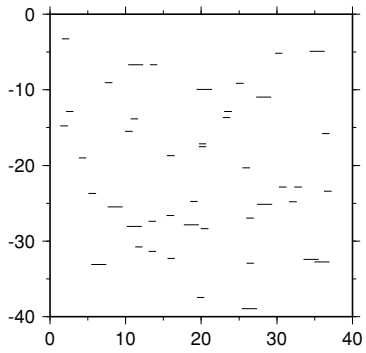

Fig. 14. Same as those in Fig. 8 except for Model 6 ($\epsilon = 0.013$, with a free surface).

We show the results for Model 6 in Fig. 15. A noticeable feature is that the peak of Q^{-1} curve and the corner of $\Delta v/\beta$ curve are somewhat blunted because of smoothing over the different crack lengths. Except for that, we again recognize the relatively good agreement between the theoretical and experimental results. This suggests the validity of the theory, even for mixed cracks with different sizes, as well as the validity of the superposition principle assumed. We also remark that Suzuki (2004) made a similar experiment on cracks with the lengths varying more smoothly and obtained a consistent result. Those may probably be the first

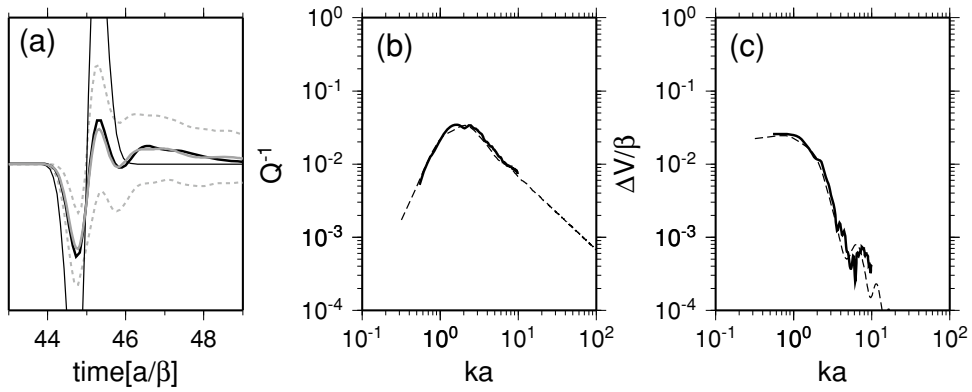

Fig. 15. Same as those in Fig. 11 except for Model 6. Note that a denotes the mean crack length only in this case.

examples of validating the Foldy approximation theory for multi-scale scatterers.

6. Discussion and Conclusions

In this paper, we applied a standard fourth-order velocity-stress FDM to the simulations of SH waves scattered by 2-D parallel cracks. We expressed traction-free cracks on the finite-difference grid in probably the simplest manner, i.e, assuming arrays of grid points with zero traction. We performed two types of accuracy tests of the method, on the basis of comparison with a reliable BIEM; one is the calculation of the displacement discontinuity along an isolated crack acted on by harmonic waves, and the other is synthesizing seismograms of waves scattered by several clustered cracks at somewhat distant stations. Both tests suggest that the fourth-order FDM yields practically sufficient accuracy, except for the wavefields in the very vicinity of cracks, which can be well described by the second-order FDM.

The present method has some advantages over the BIEM. First of all, it has no limitation with respect to the variation of crack lengths, as we demonstrated above. Also mentioned in Subsection 3.2, it could be more cost-effective when dealing with many densely distributed cracks, though the quantitative conclusions depend on many factors such as required accuracy. The most remarkable merit of the FDM would be, however, the ability to incorporate the background heterogeneity in a straightforward manner. This would be the point that the BIEM is weak, since it is essentially applicable only to structures with their Green functions known. Although we did not show any examples here, the FDM could be readily applied to many seismological problems, such as waves trapped by a fault zone made of weak materials with many fractures. We also remark that the extensions of the present method concerning 2-D SH wave scattering to other types of waves is almost straightforward; the extension to P-SV waves in 2-D cracked media will be demonstrated in our next paper, as mentioned in Section 1.

On the other hand, the present method can deal with rather limited types of cracks, as the price of its high simplicity. For instance, only the cracks parallel to the grid lines (x- or z-directions) can be exactly (in the discretized numerical sense) treated by the present method. Incorporation of inclined cracks into the grid retaining the computational accuracy, remains to be investigated. One of the candidates for inclined cracks is the use of stairsteps of FDM grids; the stairstep approximation has been successfully applied to the fluid-solid boundary with tangential discontinuity (e.g., van Vossen *et al.*, 2002; Okamoto and Takenaka, 2005).

The present method has also been validated only for cracks with the traction-free condition, namely, empty cracks. They are not, of course, realistic in the crust. Thus the extensions of the method with respect to these points is required. For handling more general crack boundary conditions, the approach of Fehler and Aki (1978) might be useful. For evaluating the diffraction by a single crack filled with compressible inviscid fluid, they defined the boundary condition as the constitutive relation with respect to the displacement discontinuity and the resistance by the internal fluid, which was successfully solved using the FDM. We remark that it is essentially the same as the manner of Kawahara and Yamashita (1992) to deal with a crack filled with incompressible viscous fluid, that was adopted in the BIEM simulations of Murai *et al.* (1995). We therefore infer that general compressible viscous fluid could be also treated in the same manner.

As an application of this method, we performed the simulations of wave propagation in media with randomly distributed cracks of the same length. We experimentally determined the attenuation and velocity dispersion induced by scattering from synthetic seismograms, using a waveform averaging technique. It was shown that the results are well explained by the theory of Kawahara and Yamashita (1992) based on the Foldy approximation for crack densities up to about 0.1. The presence of a free surface does not affect the validity of the theory. An additional experiment also suggests that the validity will be unchanged, even for cracks with varying lengths. Note that the theory has also been verified with regard to 2-D SH wave scattering by cracks filled with viscous liquid (Murai *et al.*, 1995). In addition, we will validate the theory in the case of P-SV wave scattering by 2-D cracks (Kawahara, 1992) in our next paper. All these results strongly suggest the universal validity of the Foldy approximation theory independently of the types of cracks and waves, as long as its precondition (i.e., the assumption of random sparse distributions) is satisfied.

Acknowledgments. We deeply appreciate Yoshio Murai for providing his BIEM code that is essential to the accuracy tests we carried out. The comments of Eiichi Fukuyama, Haruo Sato, and an anonymous reviewer helped us to improve the manuscript. All the figures in this paper were generated using the GMT software of Wessel and Smith (1998). This study was partially supported by the Earthquake Research Institute Cooperative Research Program (2000-B-07, 2003-B-04).

References

Aki, K. and P. G. Richards, *Quantitative Seismology*, 2nd edition, 699 pp., University Science Books, Sausalito, California, 2002.

Benites, R., K. Aki, and K. Yomogida, Multiple scattering of SH waves in 2-D media with many cavities, *Pure Appl. Geophys.*, **138**, 353–390, 1992.

Benites, R., P. M. Roberts, K. Yomogida, and M. Fehler, Scattering of elastic waves in 2-D media I. Theory and test, *Phys. Earth Planet. Inter.*, **104**, 161–173, 1997.

Bouchon, M., Diffraction of elastic waves by cracks or cavities using the discrete wavenumber method, *J. Acoust. Soc. Am.*, **81**, 1671–1676, 1987.

Clayton, R. and B. Engquist, Absorbing boundary conditions for acoustic and elastic equations, *Bull. Seism. Soc. Am.*, **67**, 1529–1540, 1977.

Coates, R. T. and M. Schoenberg, Finite-difference modeling of faults and fractures, *Geophysics*, **60**, 1514–1526, 1995.

Coutant, O., Numerical study of the diffraction of elastic waves by fluid-filled cracks, *J. Geophys. Res.*, **94**, 17805–17818, 1989.

Crampin, S., The fracture criticality of crustal rocks, *Geophys. J. Int.*, **118**, 428–438, 1994.

Fehler, M. and K. Aki, Numerical study of diffraction of plane elastic waves by a finite crack with application to location of a magma lens, *Bull. Seism. Soc. Am.*, **68**, 573–598, 1978.

Foldy, L. L., The multiple scattering of waves. I. General theory of isotropic scattering by randomly distributed scatterers, *Phys. Rev.*, **67**, 107–119, 1945.

Frankel, A., A review of numerical experiments on seismic wave scattering, *Pure Appl. Geophys.*, **131**, 639–685, 1989.

Gibson, B. S. and A. R. Levander, Apparent layering in common-midpoint stacked images of two-dimensionally heterogeneous targets, *Geophysics*, **55**, 1466–1477, 1990.

Hong, T.-K. and B. L. N. Kennett, On a wavelet-based method for the numerical simulation of wave propagation, *J. Comp. Phys.*, **183**, 577–622, 2002.

Hudson, J. A., A higher order approximation to the wave propagation constants for a cracked solid, *Geophys. J. Roy. Astr. Soc.*, **87**, 265–274, 1986.

Ikelle, L. T., S. K. Yung, and F. Daube, 2-D random media with ellipsoidal autocorrelation functions, *Geophysics*, **58**, 1359–1372, 1993.

Ishimaru, A., *Wave Propagation and Scattering in Random Media*, Vols. 1 and 2, 609 pp., Academic Press, New York, 1978 (reissued in 1997 by IEEE Press and Oxford Univ. Press, New York).

Jannaud, L. R., P. M. Adler, and C. G. Jacquin, Spectral analysis and inversion of codas, *J. Geophys. Res.*, **96**, 18215–18231, 1991a.

Jannaud, L. R., P. M. Adler, and C. G. Jacquin, Frequency dependence of the Q factor in random media, *J. Geophys. Res.*, **96**, 18233–18243, 1991b.

Kawahara, J., Scattering of P, SV waves by a random distribution of aligned open cracks, *J. Phys. Earth*, **40**, 517–524, 1992.

Kawahara, J. and T. Yamashita, Scattering of elastic waves by a fracture zone containing randomly distributed cracks, *Pure Appl. Geophys.*, **139**, 121–144, 1992.

Keller, J. B., Stochastic equations and wave propagation in random media, *Proc. Symp. Appl. Math.*, **16**, 145–170, 1964.

Kelner, S., M. Bouchon, and O. Coutant, Numerical simulation of the propagation of P waves in fractured media, *Geophys. J. Int.*, **137**, 197–206, 1999.

Kikuchi, M., Dispersion and attenuation of elastic waves due to multiple scattering from inclusions, *Phys. Earth Planet. Inter.*, **25**, 159–162, 1981a.

Kikuchi, M., Dispersion and attenuation of elastic waves due to multiple scattering from cracks, *Phys. Earth Planet. Inter.*, **27**, 100–105, 1981b.

Levander, A. R., Forth-order finite-difference P-SV seismograms, *Geophysics*, **53**, 1425–1436, 1988.

Liu, E. and Z. Zhang, Numerical study of elastic wave scattering by cracks or inclusions using the boundary integral equation method, *J. Comp. Acoust.*, **9**, 1039–1054, 2001.

Madariaga, R., Dynamics of an expanding circular fault, *Bull. Seism. Soc. Am.*, **66**, 639–666, 1976.

Main, I. G., S. Peacock, and P. G. Meredith, Scattering attenuation and the fractal geometry of fracture systems, *Pure Appl. Geophys.*, **133**, 283–304, 1990.

Mal, A. K., Interaction of elastic waves with a Griffith crack, *Int. J. Engng. Sci.*, **8**, 763–776, 1970.

Muir, F., J. Dellinger, J. Etgen, and D. Nichols, Modeling elastic fields across irregular boundaries, *Geophysics*, **57**, 1189–1193, 1992.

Müller, T. M. and S. A. Shapiro, Most probable seismic pulses in single realizations in two- and three-dimensional random media, *Geophys. J. Int.*, **144**, 83–95, 2001.

Murai, Y., J. Kawahara, and T. Yamashita, Multiple scattering of SH waves in 2-D elastic media with distributed cracks, *Geophys. J. Int.*, **122**, 925–937, 1995.

Okamoto, T. and H. Takenaka, Fluid-solid boundary implementation in the velocity-stress finite-difference method, *Zisin* (*J. Seism. Soc. Japan*), **57**, 355–364, 2005 (in Japanese with English abstract and figures)

Pointer, T., E. Liu, and J. A. Hudson, Numerical modelling of seismic waves scattered by hydrofractures: application of the indirect boundary element method, *Geophys. J. Int.*, **135**, 289–303, 1998.

Roth, M. and M. Korn, Single scattering theory versus numerical modelling in 2-D random media, *Geophys. J. Int.*, **112**, 124–140, 1993.

Saenger, E. H. and S. A. Shapiro, Effective velocities in fractured media: a numerical study using the rotated staggered finite-difference grid, *Geophys. Prospect.*, **50**, 183–194, 2002.

Saenger, E. H., N. Gold, and S. A. Shapiro, Modeling the propagation of elastic waves using a modified finite-difference grid, *Wave Motion*, **31**, 77–79, 2000.

Saenger, E. H., O. S. Krüger, and S. A. Shapiro, Modeling the propagation of elastic waves using a modified finite-difference grid, *Geophys. Prospect.*, **52**, 183–195, 2004.

Saito, T., H. Sato, M. Fehler, and M. Ohtake, Simulating the envelope of scalar waves in 2D random media having power-law spectra of velocity fluctuation, *Bull. Seism. Soc. Am.*, **93**, 240–252, 2003.

Samuelides, Y. and T. Mukerji, Velocity shift in heterogeneous media with anisotropic spatial correlation, *Geophys. J. Int.*, **134**, 778–786, 1998.

Sato, H. and M. C. Fehler, *Seismic Wave Propagation and Scattering in the Heterogeneous Earth*, 308 pp., Springer-Verlag, New York, 1998.

Suzuki, Y., Simulations of seismic waves scattered by 2-D cracks using the finite difference method, MSc thesis, Ibaraki University, Mito, 2004 (in Japanese).

Van Antwerpen, V. A., W. A. Mulder, and G. C. Herman, Finite-difference modeling of two-dimensional elastic wave propagation in cracked media, *Geophys. J. Int.*, **149**, 169–178, 2002.

Van Baren, G. B., W. A. Mulder, and G. C. Herman, Finite-difference modeling of scalar-wave propagation in cracked media, *Geophysics*, **66**, 267–276, 2001.

Van Vossen, R., J. O. A. Robertsson, and C. H. Chapman, Finite-difference modeling of wave propagation in a fluid-solid configuration, *Geophysics*, **67**, 618–624, 2002.

Viriuex, J., SH-wave propagation in heterogeneous media: velocity-stress finite difference method, *Geophysics*, **49**, 1933–1957, 1984.

Vlastos, S., E. Liu, I. G. Main, and X.-Y. Li, Numerical simulation of wave propagation in media with discrete distributions of fractures: effects of fracture sizes and spatial distributions, *Geophys. J. Int.*, **152**, 649–668, 2003.

Wessel, P. and W. H. F. Smith, New, improved version of the Generic Mapping Tools Released, *EOS, Trans., Am., Geophys. Un.*, **79**, 579, 1998.

Yamashita, T., Attenuation and dispersion of SH waves due to scattering by randomly distributed cracks, *Pure Appl. Geophys.*, **132**, 545–568, 1990.

Yomogida, K. and R. Benites, Scattering of seismic waves by cracks with the boundary integral method, *Pure Appl. Geophys.*, **159**, 1771–1789, 2002.

Zhang, Ch. and D. Gross, *On Wave Propagation in Elastic Solids with Cracks*, 248 pp., Computational Mechanics, Southampton, UK, 1997.

Y. Suzuki, J. Kawahara (e-mail: junk@mx.ibaraki.ac.jp), T. Okamoto, and K. Miyashita